Experimental and Numerical Behavior of Horizontally Loaded Piled Rafts with a Defective Pile

Francisco Javier Alva García
University of Brasilia: Universidade de Brasilia
Renato Pinto da Cunha
University of Brasilia: Universidade de Brasilia
Paulo José Rocha de Albuquerque
State University of Campinas: Universidade Estadual de Campinas
Márcio Muniz de Farias
University of Brasilia: Universidade de Brasilia
Heitor Cardoso Bernardes (heitor.bernardes@ifgoiano.edu.br)
University of Brasilia: Universidade de Brasilia

Research Article

Keywords: defective pile, piled raft, horizontal load, finite element analysis.

Posted Date: March 29th, 2022

DOI: https://doi.org/10.21203/rs.3.rs-1450058/v1

Abstract

The present paper aims to investigate the effects of defective piles in horizontally loaded piled raft foundations. Close to real scale foundation models of defective and intact three-piled systems were submitted to horizontal load tests. The models used bored type piles drilled with 5 m in length and 0.25 m in diameter, connected to a concrete raft founded on a tropical soil profile at the University of Campinas research site. Based on the experimental data, a tridimensional finite element analysis was initially calibrated and consequently used to study the effects of the defective element at the pile load distribution and the horizontal subgrade forces at the pile shaft. The results show that the presence of a defective pile increases the raft tilting, which affects both vertical and horizontal load distributions among the raft and the piles, and among trailing and leading piles.

1. Introduction

The concept of deep foundations enhanced with a raft element in full contact with the soil has received considerable attention in recent years for the foundation design of buildings subjected to high horizontal loadings, such as onshore wind turbines (Ravichandran et al. 2018; Shrestha et al. 2018) and pencil towers (Poulos 2016). However, when dealing with horizontally loaded structures, the friction resistance at the raft-soil interface is not the only factor responsible for the superior performance of piled rafts over “conventional” pile groups. One shall remind that conventional groups are those designed without consideration on the raft-soil contact.

Unsever et al. (2015) showed using 1g small-scale models and tridimensional finite element analysis (3D FEA) that the higher contact pressures, which the raft transfer to the ground, increase the stiffness and the strength of the soil surrounding the piles, improving their behavior.

On the other hand, centrifuge tests in piled raft models indicate that as the magnitude of the horizontal load increases, so do the pile loads, which causes a constraining effect in the upper soil beneath the raft, reducing its shear deformation and consequently the mobilized shear stresses at the raft-soil interface (Horikoshi et al. 2003).

These aspects show the complexity of predicting the behavior of horizontally loaded piled rafts, whose behavior in field conditions will depend on a series of factors, of which one can highlight the mechanical properties of the soil, and the geometric characteristics of the foundation, such as the dimensions and spacing of the piles and the raft, and other aspects that are addressed in different papers (Zhang and Small 2000; Kitiyodom and Matsumoto 2002, 2003; Rollins and Sparks 2002; Sawada and Takemura 2014; Kavitha et al. 2016; Cunha and Poulos 2018; Stacul 2018; Kumar and Vasanwala 2021; Rosendo and Albuquerque 2021).

However, given unfavorable soil or installation conditions, a certain level of damage might develop in the piled system. This may happen both in driven precast piles, as fissuring on the concrete due to the

constant hammering on the cap, and in cast in place piles, as necking, soil inclusion, ‘soft toe’ conditions, and other integrity problems caused by a poor drilling technique (Karandikar 2018).

Despite the continuous advances in pile integrity tests and foundation quality control (Zhussupbekov and Omarov 2016; Hannigan and Piscsalko 2021), many cases of defective piles cannot be readily identified, that eventually may alter the foundation designed behavior. Some research has been already done to investigate the effects of defective piles in piled rafts and pile groups subjected to vertical loads (Albuquerque et al. 2017; Freitas Neto et al. 2020; Cunha et al. 2021), but in cases involving horizontally loaded piled foundations, the scientific literature is scarce.

This paper therefore investigates the effects of defective piles in laterally loaded piled raft foundations. With this objective, two three-piled rafts founded on a tropical soil profile at the research site of the University of Campinas were executed, and subjected to horizontal load tests to failure. The piles were drilled with 5 m in depth and 0.25 m in diameter, with 1.25 m spacing (axis to axis). In one of the tested foundations, one of the piles had a damaged region, which was specifically designed to simulate a structural defect. The tests were analyzed using 3D FEA, which allowed to understand the system’s mechanics in terms of load distribution, raft tilting, and horizontal subgrade reactions among trailing and leading piles.

2. Materials And Methods

2.1 Experimental Program

Horizontal load tests were carried out at the experimental research site of the University of Campinas (Unicamp) in the city of Campinas (Sao Paulo, Brazil). The geotechnical profile consists of a 2 m thick layer of very soft silty clay overlying 6 m thick silty sand strata of low to medium (increasing) compacity. The bedrock is made of a fractured Diabase, from 8 m deep onwards. The main geotechnical properties obtained from physical characterization tests and consolidated undrained triaxial compression tests (Gon 2011) are shown in Table 1.

Table 1
Typical geotechnical parameters from the research site (Freitas Neto 2013).

Depth (m)	USCS	γ_{nat} (kN/m^3)	w (%)	E_s (MPa)	c' (kPa)	ϕ' (º)
1.00	MH	14.1	28.3	13.8	7.4	22
2.00	ML	14.2	27.9	11.4	7.8	21
3.00	ML	14.0	28.0	8.5	11.6	22
4.00	ML	14.4	25.5	11.5	5.7	23
5.00	ML	15.5	26.2	9.9	24.0	21
6.00	ML	15.3	26.1	19.9	42.4	22
7.00	ML	15.4	28.3	10.9	41.9	22
8.00	MH	15.2	32.3	11.0	26.4	22

USCS: Unified soil classification system; MH: High compressibility silt; ML: Low compressibility silt; γ_{nat}: Soil specific weight in natural conditions; w: Moisture content; E_s : Soil Young's modulus; c': Soil effective cohesion; ϕ': Soil effective friction angle.

Two horizontal load tests were carried out in three-piled rafts, with pile spacing equal to 1.25 m. The foundations were composed of bored piles, with 5 m in length and 0.25 m in diameter, as shown in Fig. 1a. After the pile installation, the raft steel reinforcement was placed and the fluid concrete was poured against the soil to ensure a full raft-soil contact during the tests.

Figure 1b shows the horizontal load tests apparatus, in which is possible to notice the excavation of the soil around the lateral of the raft, to avoid the influence of any sort of passive earth pressure reaction. The experimental testing setup and load sequence were carried out in accordance with the Brazilian Standard NBR 12131 (ABNT 2006). The tests were slow maintained, with a semi-static increasing load sequence using a 15 kN load increase at each stage. A 200 kN load cell was used to monitor the applied horizontal force and four 0.01 mm dial gauges were placed for the measurements of the raft tilt and horizontal displacements.

One of the tested foundations had all its three piles intact (CC3) and the other had one of the piles with a damaged region (CF3), with the aim to simulate a pile's shaft region with structural breakage, as shown in Figs. 2a and 2b. The damaged zone consisted of a hollow concrete region, with 0.245 m in external diameter and 0.195 m in internal diameter, concreted with a low resistance concrete, whose compressive strength was computed from several resistance compression tests done by a previous doctoral thesis (Freitas Neto 2013). The pile defective section was 0.60 m long and without steel reinforcement, as shown in Fig. 2b. The damaged section was expected to, and indeed broke, during the load tests.

The pile defect was intentionally located at 8 pile diameters below the soil surface, which is the typical zone where a plastic hinge may eventually form, and a crack might develop within the pile's shaft from

laterally loaded foundation structures. This hypothesis was confirmed after the pile's exhumation.

2.2 Numerical Modelling

To allow a better understanding of the effects of the defective pile in different aspects of the piled raft behavior, such as pile load distribution, raft tilting, and the mechanisms of geotechnical failure, the tests were analyzed using a 3D finite element model, developed using the software Abaqus. To simulate the pile behavior and its structural failure, the numerical model included the simulation of the soil dominium and the foundation structural components.

A damaged plasticity constitutive model was employed to simulate the concrete and an elastic-perfectly plastic model was used to simulate the steel's stress-strain behavior. A perfect bond was assumed at the interface between the concrete and the steel reinforcement. Table 2 shows the main mechanical parameters of these materials. The other parameters of the damaged plasticity model were null, i.e., eccentricity, viscosity, the ratio of biaxial to the uniaxial compressive yield stresses, and the ratio of the second stress invariant on the tensile meridian to that on the compressive meridian.

Table 2
Parameters used for the concrete and steel reinforcement in the numerical model.

Concrete	**γ_c (kN/m^3)**	***fck* (MPa)**	**E_c (GPa)**	**v_c**	**Dilation Angle**
Raft and piles	21.6	36.7	45.0	0.2	15°
Pile (defective zone)	21.6	2.0	5.9	0.2	15°
Steel reinforcement	γ_y (kN/m^3)	*fyk* (MPa)	E_y (GPa)	v_y	Diameter (mm)
Rods and stirrups	77.0	500.0	231.0	0.3	10.0 (rods) and 6.3 (stirrups)

γ_c and γ_y: Specific weight of the concrete and the steel, respectively; E_c and E_y: Young's modulus of the concrete and the steel, respectively; v_c and v_y: Poisson's ratio of the concrete and the steel, respectively; *fck* is the characteristic compressive strength of the concrete, and *fyk* is the characteristic yield strength of the steel.

An elastic-perfectly plastic model with the Mohr-Coulomb failure criteria was used to model the soil. The model was initially calibrated using the soil strength and stiffness parameters presented in Table 1. Then, based on those initial results, a subsequent back analysis procedure was carried out, with the aim of a closer match between experimental results and numerical predictions.

It is important to highlight that several unknown factors might be somehow involved during the lateral loading, such as soil anisotropy, variation in soil moisture in shallow depths, and the loss of the original soil structure during pile installation. However, these factors are intrinsically shown in the obtained

experimental curves, and for this reason, the back analysis procedure is a reasonable approach to calibrate the numerical model.

After the numerical procedure, the final geotechnical parameters were obtained, as shown in Table 3. The soil's Poisson's ratio (v_s), dilation angle (ψ_s) and coefficient of earth pressure at rest (k_0) were equal to $v_s = 0.3$, $\psi_s = 0$ and $k_0 = 0.4$ in all soil layers. The interface between the pile's shaft and the surrounding soil was considered using the β method (Burland 1973), which unit shaft resistance (f_s) values for each layer are shown in Table 3. The contact between the raft's base and the underlying ground was considered, using a frictional coefficient of 0.15 without any maximum shear stress limit.

Table 3
Geotechnical parameters used in the numerical simulations.

Layer	Thickness (m)	E_s (MPa)	c (kPa)	ϕ (^{o})	fs (kPa)
1	0.45	49.6	7.4	22	2.56
2	1.00	41.1	7.8	21	3.54
3	10.55	36.0	13.8	22	11.63

The numerical analyses were performed using an incremental procedure to the horizontal load advance. Since the analysis involves a highly nonlinear behavior, with significant changes in the structure stiffness matrix, the Riks method was applied.

3. Results And Discussion

Figure 3 shows the load-displacement curves obtained for the CC3 and CF3 tests. Considering the displacement failure criteria (10% of pile diameter, i.e. 25 mm), the foundation ultimate capacity (Q_{ult}) of the systems CC3 and CF3 were defined as 188 and 122 kN, respectively, which corresponds to a reduction of approximately 35% in the load capacity of the defective system.

The results in Fig. 3 also show good agreement between experimental and numerical curves. The back-analyzed parameters used to adjust the numerical prediction were able to capture both foundation stiffness and geotechnical failure. The software graphical output (Fig. 4) shows the formation of passive lateral earth pressure wedges (along soil's surface) for both leading and trailing piles in the final steps, close to the overall soil failure.

The horizontal displacement contour map in Fig. 4 shows that the leading pile sustained most of the mobilized horizontal reaction. The plot also shows the importance of a reliable characterization of the soil upper layers, since the horizontal displacements were confined to a soil depth equal to 5–6 times the pile diameter. Both aspects are in accordance with the findings of Reese and Van Impe (2001). A gaping

zone in the back part of the trailing piles is also noticed, indicating the actual separation that takes place between the soil-pile interfaces as the system approaches geotechnical failure.

Once the model was calibrated, it was possible to estimate output system variables that could not be measured during the experimental program. Hence, the numerical predictions of the pressure mobilized at each pile's base, the raft tilting, the raft-soil contact normal forces, and the unit horizontal subgrade force at the borehole's surface.

3.1 Mobilized pressure at the pile base, raft tilting, and raft-soil contact normal forces

The results of the numerically computed pressure at each pile base (P_i) were normalized in relation to maximum unit bearing pressure at the tip of the respective pile (P_{imax}). The results are shown in Fig. 5, for increasing values of the applied horizontal load (Q_h), from 20–100% of the horizontal failure load (Q_{ult}). The Q_{ult} value applied to the normalized Q_h was the one obtained from the defective system (CF3), in which Q_{ult} = 122 kN.

Figure 5 shows that despite the presence of a damaged zone, the defective pile continued to absorb and transmit a percentage of vertical load to its base. The results show a migration of vertical load from the trailing piles (piles 2 and 3) to the leading one (pile 1) when the system is defective, due to its tilting. This phenomenon is very contrasting when compared to the intact case system, which indicated a different distribution of loads between leading and trailing piles, establishing a more homogeneous distribution than the defective system.

For both CC3 and CF3 systems, the P_{imax} values of the leading pile (P_{1max}) were around 10 to 16 times the values for the piles 2 and 3 (P_{2max} and P_{3max} – the trailing ones); the latter, in turn, presented very similar values between them, even in the defective system.

To understand the reason of the load spread that occurred by the presence of the defective pile, the raft's tilting at each loading stage has to be assessed. Figure 6a shows the numerically derived tilt angle (ψ), normalized to its maximum value (ψ_{max}), developed at the system's ultimate load stage. The results show a relation between tilting and load migration to the leading pile tip in both defective and intact systems. Indeed, the increase in foundation tilting when the CF3 system is submitted to a horizontal loading between 40% and 80% of Q_{ult}, explains the load migration from trailing piles to the leading one (Pile 1) – as depicted in Fig. 5.

It shall be noticed that the relative tilting was much greater for the defective system than for the intact one, which was already expected given the influence of the defective trailing pile. This greater tilting was responsible for almost zeroing the unit bearing pressure for trailing pile 3 in the defective system (Fig. 5). On the other hand, in the intact system, this same pile still carried vertical load until the latest loading level.

Figure 6b shows the raft-soil normal force ($q_{rs\,i}$), acting in two opposite nodes at the raft soil interface (points T and L in Fig. 6b). The results are normalized in relation to its maximum value ($q_{rs\,max}$), which was measured in point L of the intact system (CC3). The results show that the presence of the defective pile caused a large decrease in the contact normal forces acting in the leading pile region (CF3 – Point L), to approximately 40% of the value computed in the intact system. This aspect will reduce the contribution of the raft-soil interface to absorb horizontal loadings.

Another interesting aspect shown in Fig. 6b is the decrease of the q_{rs} value acting at the point T (CC3 system), which occurs until approaching null values, at 60% of Q_{ult}. In the defective system, the same point showed negligible values of q_{rs} during all stages of the horizontal loading. This behavior corroborates with a high tilt verified to the CF3 system (Fig. 6a), and shows the large impact that the defective pile can cause on the effectiveness of the use of the raft-soil interface to absorb horizontal loads – hence the design as a piled raft.

3.2 Unit Horizontal Subgrade Force at Borehole's Surface

The pile's shaft-soil interaction was analyzed using the unit horizontal subgrade (reaction) forces acting on both front and back surface positions of the borehole, at several depths of interest along with the pile's depth. The unit horizontal subgrade force (q_{iwl}) was normalized by its respective maximum value ($q_{iwl\,max}$) developed throughout the analyzed loading stage.

Figure 7 shows the normalized horizontal subgrade forces for pile 1 (Fig. 7a), 2 (Fig. 7b), and 3 (Fig. 7c). The results were solely computed to the allowable displacement level (working condition), i.e., the horizontal load corresponding to a horizontal displacement level equal to 5% of the pile diameter (design assumption). In the plot, positive signs indicate compression forces in the same direction as the horizontal loading onto the raft, whereas a negative sign means compression forces acting in the opposite direction. In both cases, the unit subgrade reactions at both borehole's front and back surface positions are originated from the passive earth pressure caused by the interaction between the piles and the surrounding soil.

The results show that the reaction subgrade forces tend to be higher at the front surface position for the first 2 m (8 times the pile diameter). From this depth onwards the subgrade reaction forces are greater at the back surface position, independently of the pile type (leading or trailing) and condition (intact or defective). Figure 7 also shows that depending on the pile type and on the analyzed pile depth, there was a tendency of increasing or decreasing the subgrade force when comparing the intact to the defective system case. For instance, pile 1 (leading) front surface position increased the (average) subgrade force in the pile's top region (0 to 3 m) for the defective case, when compared to similar results in the intact case.

A reverse phenomenon (decrease) was noticed for a similar comparison in the case of the trailing pile 3 in the CF3 system. Again, this was related to the migration of load and new equilibrium stage that was

accomplished by the simultaneous tilting of the raft (intact system) and tilting plus defective pile influence (defective system).

Similar to the unit base pressure, the defective trailing pile 2 continued to generate horizontal subgrade reaction forces on the surrounding borehole surface at working displacement level. Nevertheless, the effectiveness of this pile has decreased, as it generated a lower average subgrade force when compared to the same pile at the intact system condition. On the other hand, the horizontal subgrade forces distribution generated by the trailing pile 3 (intact) has not considerably change from the defective to the intact case.

At the back surface position, for both intact and defective systems, the horizontal subgrade force has zeroed for leading pile 1 and trailing pile 3, indicating the formation of a gap (as shown in Fig. 4), with total loss of contact between the pile's shaft and the borehole's surface.

4. Conclusions

An experimental and numerical study of piled raft foundations with defective piles was carried out under horizontal loading conditions, given its scarcity in literature. The defect was imposed on the upper part of the pile, in a zone where the occurrence of plastic hinges and structural failures is common. The experimental results were used to calibrate a finite element model, which allowed a detailed analysis of the effects of the defective pile on the overall foundation behavior, thus extrapolating experimental data. The main conclusions based on the study are listed as follows:

1. In horizontally loaded piled rafts, the presence of a defective pile increases the intensity of the raft tilt, causing a migration of vertical load from the trailing to the leading pile. Some migration also happens when the system is intact, given the tilting caused by the horizontal load, but in the latter case, the load distribution tends to be more homogeneous within the pile.

2. The presence of a defective pile significantly diminishes the effectiveness of the raft-soil contact in absorbing part of the applied horizontal loading, thus affecting the design when considering piled raft conditions.

3. At the back surface of the piles (either leading or trailing) the horizontal subgrade forces are null on the upper positions, indicating that a "gap" is generated with total loss of contact between the pile's shaft and the borehole. This is valid for both intact and defective systems once laterally loaded at high levels – close to herein adopted failure limits.

4. The presence of a defective pile increases the values of the horizontal subgrade forces at the upper part of the leading pile front surface (first 2 to 8 pile diameters). The opposite is true for trailing piles. In this way, the defective pile influence causes an uneven distribution of lateral forces within the foundation system that produces a torsion outcome. Depending on the load level, this particular effect needs to be structurally taken into account.

5. The present research has focused on defective piles with a narrowed structural breakage of the pile's shaft, which has been present since the beginning of the loading process. The conclusions of this study may be as well qualitatively extrapolated to other types of pile defect, with care and proper considerations (necking type flaws, short length piles and so on). The authors understand that more research is needed (and is scarce) in this field.

Declarations

Acknowledgments

This research could not have been conducted without the financial support provided by the São Paulo Research Foundation (FAPESP). The authors are also grateful for the helpful support from staff and students of the University of Campinas and University of Brasília GPFees group (https://rpcunha.wixsite.com/gpfees), at both experimental and numerical stages. The first author finally acknowledges the providential support given by the Brazilian sponsorship institution CNPq, for his doctoral scholarship.

Conflicts of interest/Competing interests: None.

Availability of data and material:

The data is from the doctoral thesis of the first author, which is available in: https://repositorio.unb.br/handle/10482/25226.

Code/Software availability:

The software license (Abaqus) was provided by the University of Brasilia.

References

1. Albuquerque PJR, Garcia JR, Freitas Neto O et al (2017) Behavioral evaluation of small-diameter defective and intact bored piles subjected to axial compression. Soils and Rocks 40:109–121. https://doi.org/10.28927/SR.402109
2. Burland JB (1973) Shaft friction of piles in clay - A simple fundamental approach. Gr Eng 6:30–42
3. Cunha RP, Cordeiro AFB, Sales MM, Bernardes HC (2021) Physical 1g Modelling of Defective Small-Scale Piled Raft Systems Founded in Sand. Int J Phys Model Geotech. https://doi.org/10.1680/jphmg.21.00025
4. Cunha RP, Poulos HG (2018) Importance of the Excavation Level on the Prediction of the Settlement Pattern from Piled Raft Analyses. Soils and Rocks 41:91–99. https://doi.org/10.28927/SR.411091
5. Freitas Neto O (2013) Experimental and Numerical Evaluation of Piled Raft with Defected Piles in Tropical Soils of Brazil. D.Sc. Thesis. Dept. of Civil and Environ. Eng., University of Brasília, Brazil, 253p (in Portuguese). Available in: https://repositorio.unb.br/handle/10482/18608

6. Freitas Neto O, da Cunha RP, Albuquerque PJR et al (2020) Experimental and numerical analyses of a deep foundation containing a single defective pile. Lat Am J Solids Struct 17:1–15. https://doi.org/10.1590/1679-78255827
7. dos Gon F (2011) S Caracterização geotécnica através de ensaios de laboratório de um solo de diabásio da região de Campinas/SP. Universidade Estadual de Campinas, Brasil, 153p, (in portuguese). Available in: http://repositorio.unicamp.br/jspui/handle/REPOSIP/258759
8. Hannigan PJ, Piscsalko G (2021) Advances in Quality Control Methods for Bored Pile and Diaphragm Wall Foundations with Case Histories. 14th Balt Sea Reg Geotech Conf - IOP Conf Ser. Earth Environ Sci 727:1–11. https://doi.org/10.1088/1755-1315/727/1/012030
9. Horikoshi K, Matsumoto T, Hashizume Y et al (2003) Performance of piled raft foundations subjected to static horizontal loads. Int J Phys Model Geotech 3:37–50. https://doi.org/10.1680/ijpmg.2003.030204
10. Karandikar DV (2018) Challenges to quality control in bored cast-in-situ piling in growing urban environment. Indian Geotech J 48:360–376. https://doi.org/10.1007/s40098-017-0277-z
11. Kavitha PE, Beena KS, Narayanan KP (2016) A review on soil-structure interaction analysis of laterally loaded piles. Innov Infrastruct Solut 1:1–15. https://doi.org/10.1007/s41062-016-0015-x
12. Kitiyodom P, Matsumoto T (2002) A simplified analysis method for piled raft and pile group foundations with batter piles. Int J Numer Anal Methods Geomech 26:1349–1369. https://doi.org/10.1002/nag.248
13. Kitiyodom P, Matsumoto T (2003) A simplified analysis method for piled raft foundations in non-homogeneous soils. Int J Numer Anal Methods Geomech 27:85–109. https://doi.org/10.1002/nag.264
14. Kumar U, Vasanwala S (2021) An Experimental Study of the Piled Raft Foundation Subjected to Combined Vertical and Lateral Load. https://doi.org/10.1007/978-981-33-6346-5_21. Geology 1–12
15. Poulos HG (2016) Tall building foundations: design methods and applications. Innov Infrastruct Solut 1:1–51. https://doi.org/10.1007/s41062-016-0010-2
16. Ravichandran N, Shrestha S, Piratla K (2018) Robust design and optimization procedure for piled-raft foundation to support tall wind turbine in clay and sand. Soils Found 58:744–755. https://doi.org/10.1016/j.sandf.2018.02.027
17. Reese LC, Van Impe WF (2001) Single piles and pile groups under lateral loading. CRC Press, London, UK
18. Rollins KM, Sparks A (2002) Lateral resistance of full-scale pile cap with gravel backfill. J Geotech Geoenvironmental Eng 128:711–723. https://doi.org/10.1061/(ASCE)1090-0241(2002)128:9(711)
19. Rosendo DC, Albuquerque PJR (2021) General analytical solution for laterally-loaded pile-based Miche model. Geotech Geol Eng 39:765–782. https://doi.org/10.1007/s10706-020-01520-1
20. Sawada K, Takemura J (2014) Centrifuge model tests on piled raft foundation in sand subjected to lateral and moment loads. Soils Found 54:126–140. https://doi.org/10.1016/j.sandf.2014.02.005

21. Shrestha S, Ravichandran N, Rahbari P (2018) Geotechnical Design and Design Optimization of a Pile-Raft Foundation for Tall Onshore Wind Turbines in Multilayered Clay. Int J Geomech 18:1–12. https://doi.org/10.1061/(ASCE)GM.1943-5622.0001061
22. Stacul S (2018) Analysis of piles and piled raft foundation under horizontal load. D.Sc. Thesis. Dept. of Arch., Civil Eng. and Environ. Sci., University of Braunschweig, Germany, 245p. http://dx.doi.org/10.24355/dbbs.084-201806181506-0
23. Unsever YS, Matsumoto T, Özkan MY (2015) Numerical analyses of load tests on model foundations in dry sand. Comput Geotech 63:255–266. https://doi.org/10.1016/j.compgeo.2014.10.005
24. Zhang HH, Small JC (2000) Analysis of capped pile groups subjected to horizontal and vertical loads. Comput Geotech 26:1–21. https://doi.org/10.1016/S0266-352X(99)00029-4
25. Zhussupbekov A, Omarov A (2016) Modern Advances in the Field Geotechnical Testing Investigations of Pile Foundations. Procedia Eng 165:88–95. https://doi.org/10.1016/j.proeng.2016.11.739
26. Brazilian Association of Technical Standards (ANBT) (2006) NBR 12131: Piles - Static load test - Test method (in portuguese). 8 p

Figures

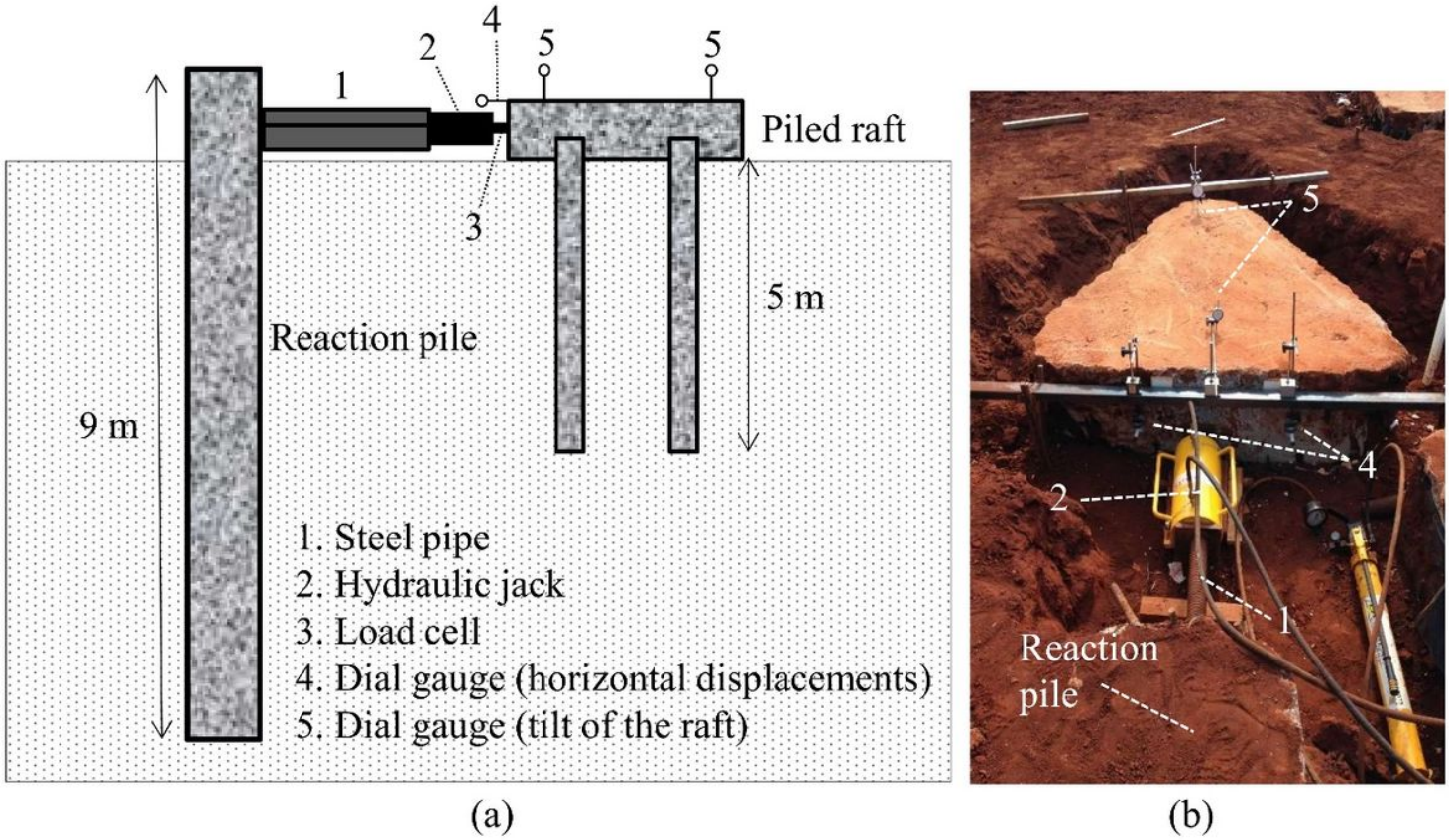

Figure 1

Horizontal load test scheme (a) and a picture of the test during its execution (b).

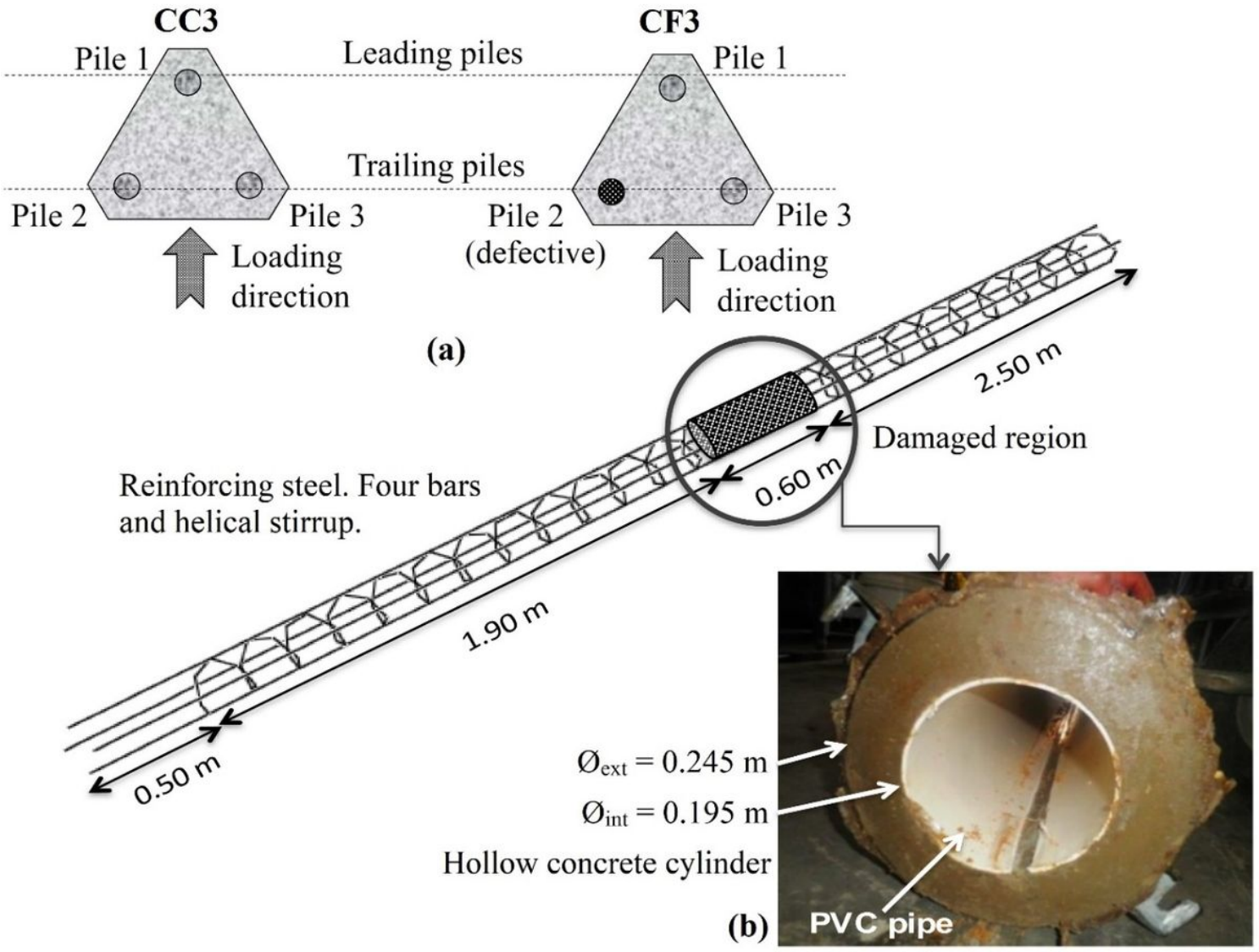

Figure 2

Intact (CC3) and defective (CF3) piled raft systems (a) and hollow concrete cylinder designed to represent the defective zone (b): modified from (Freitas Neto 2013).

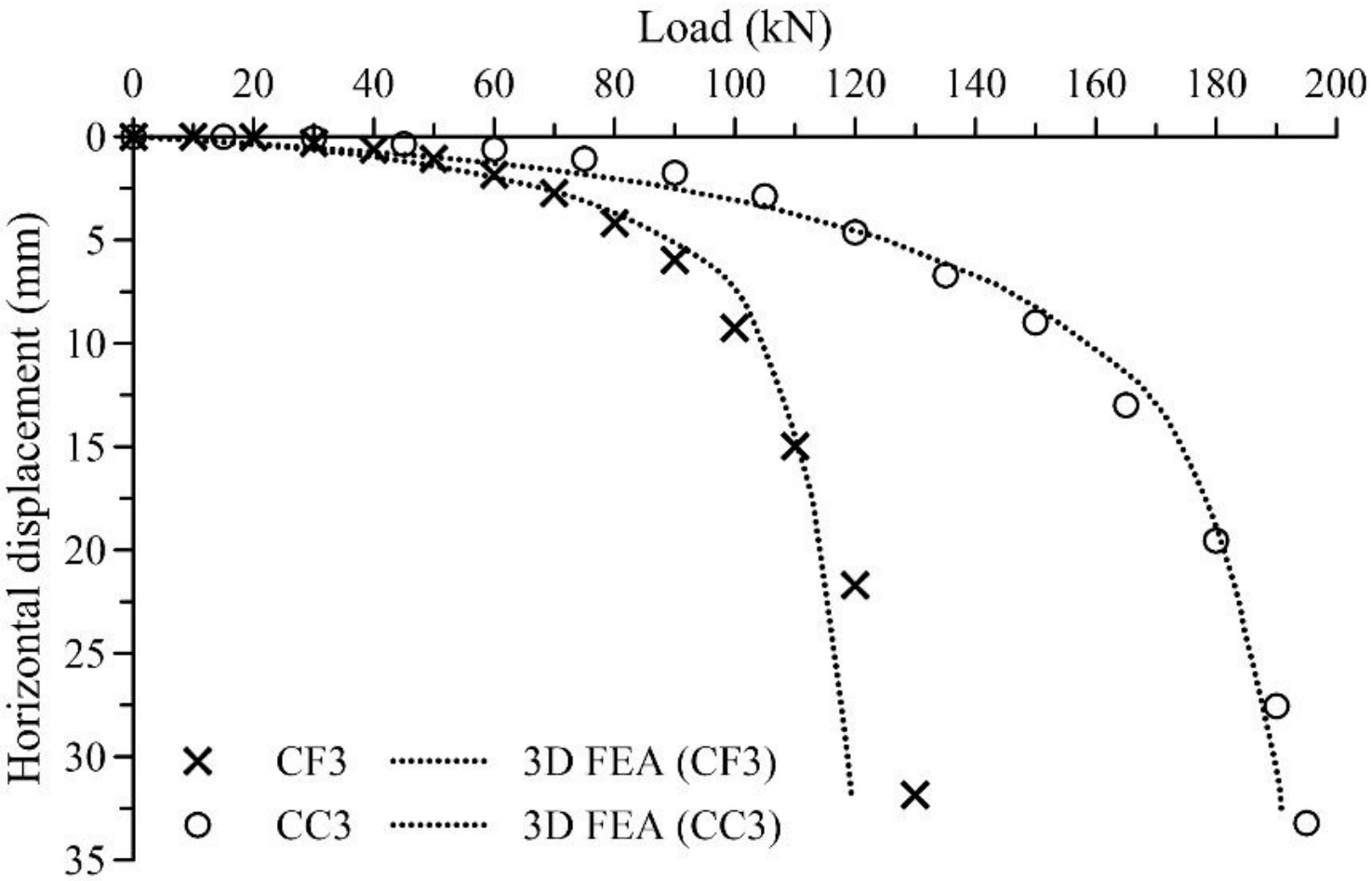

Figure 3

Load-displacement curves of the

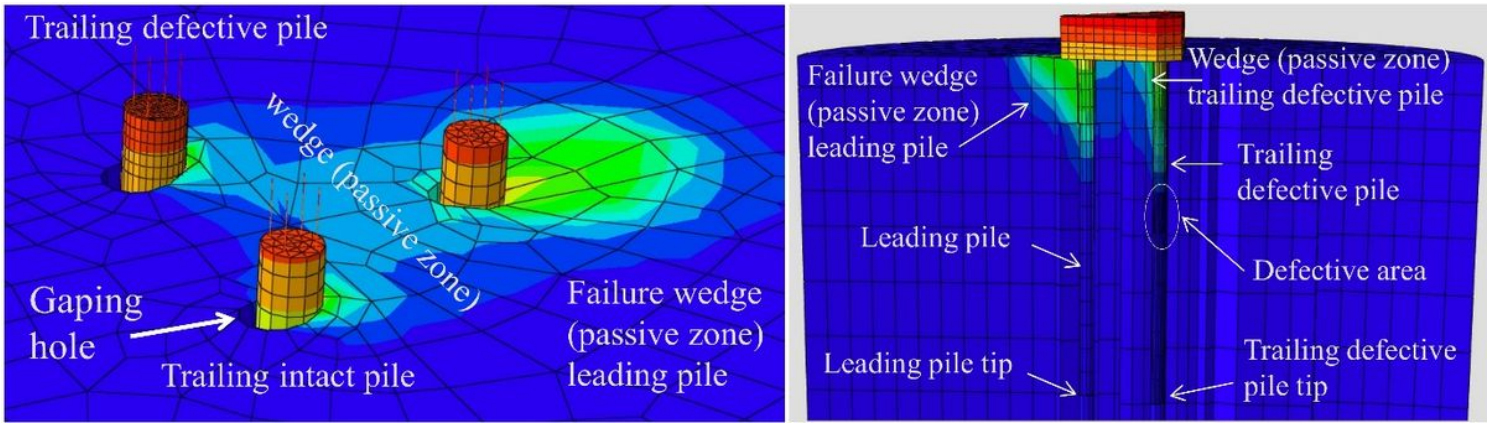

Figure 4

Horizontal displacement contour map for the CF3 system.

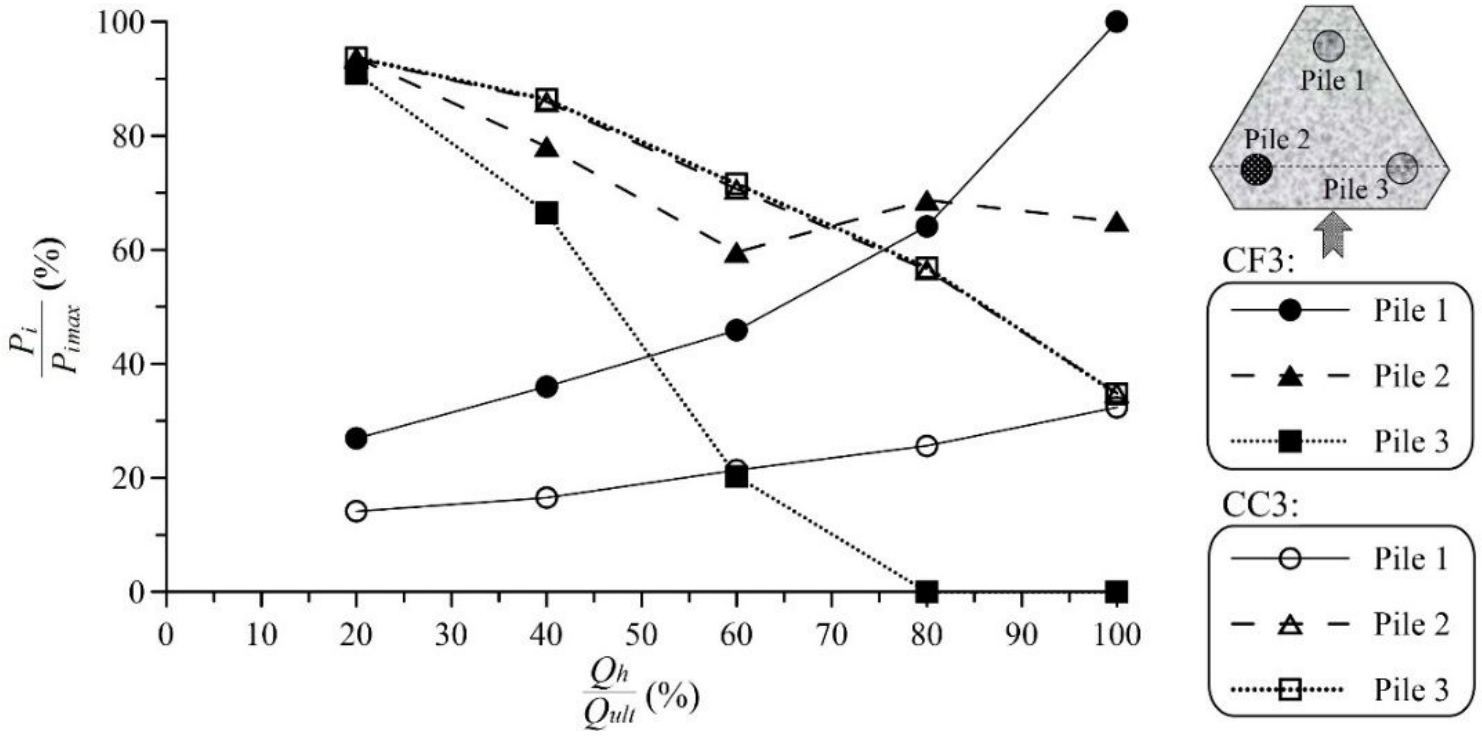

Figure 5

Normalized unit bearing pressure at each pile base for both CC3 and CF3 systems.

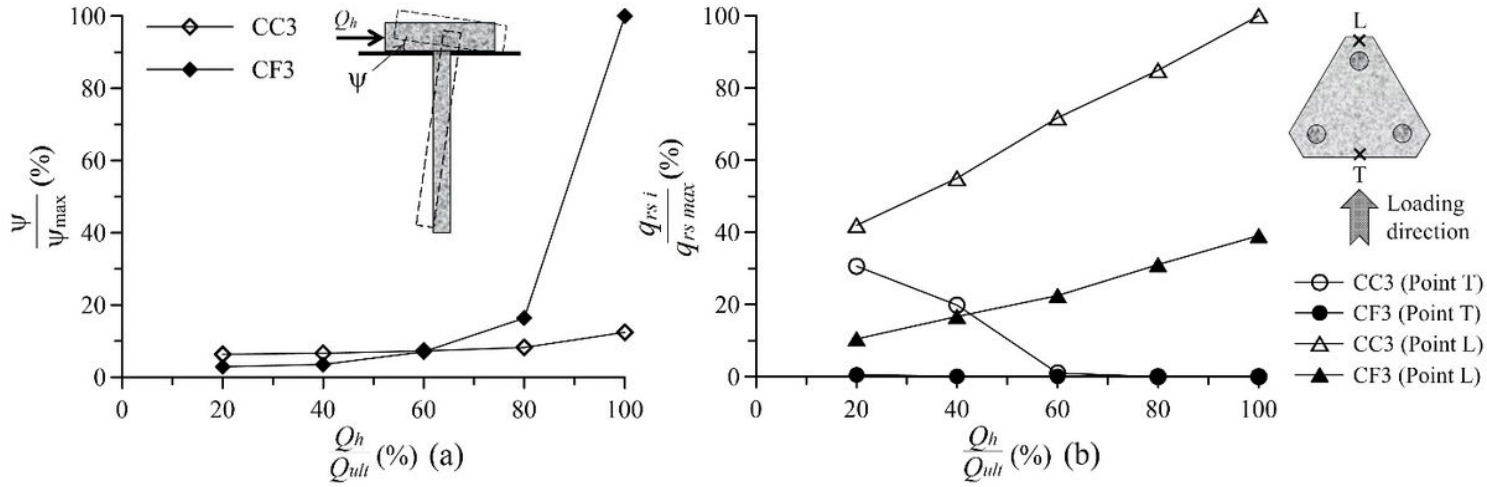

Figure 6

Normalized raft tilting (a) and raft-soil contact forces (b) for both CC3 and CF3 foundation systems.

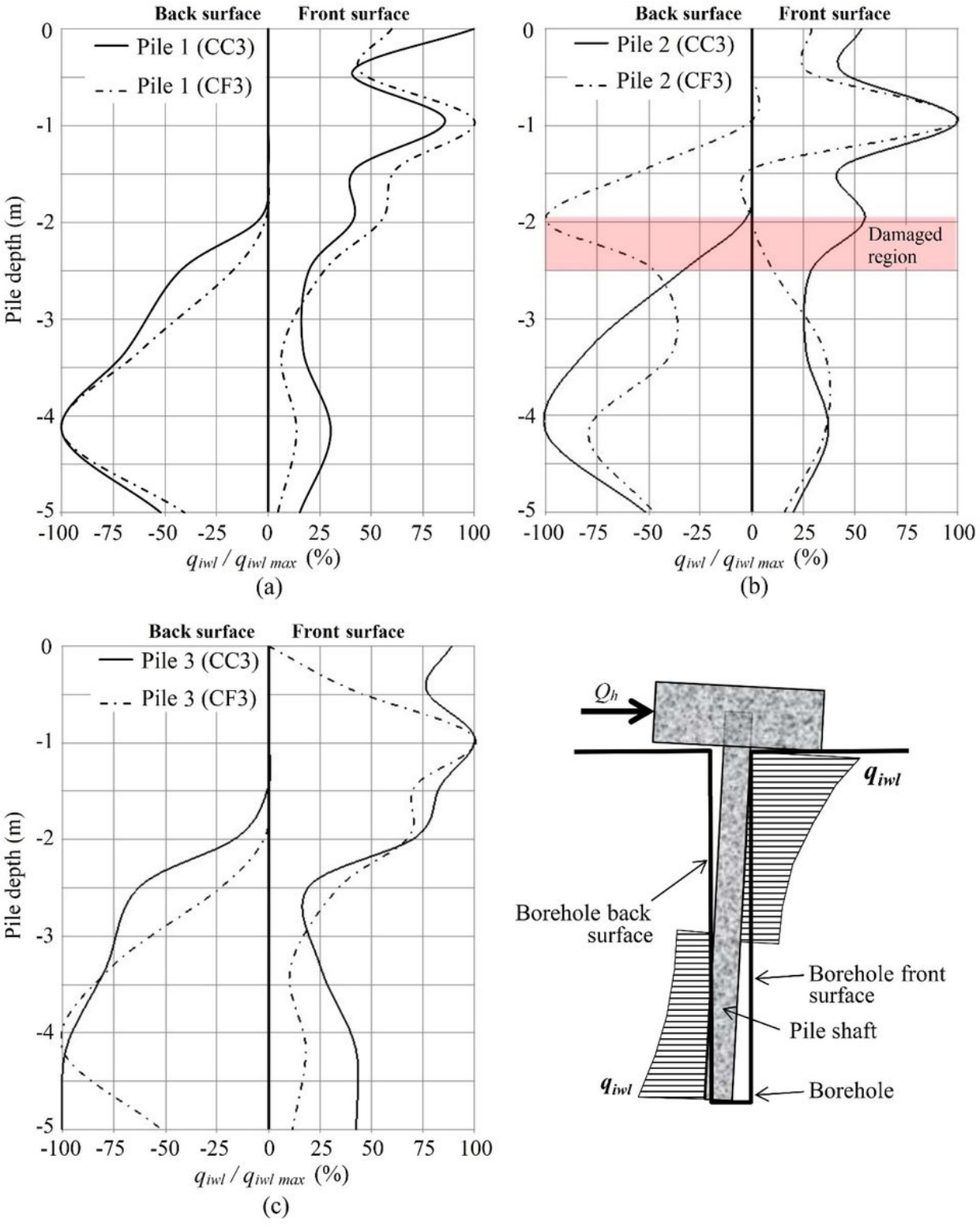

Figure 7

Normalized unit horizontal subgrade forces for piles 1 (a), 2 (b) and 3 (c) for both CC3 and CF3 systems.